Miner Deposita (2006) 41: 52–67
DOI 10.1007/s00126-005-0040-8

ARTICLE

A. F. A. Marques · F. Barriga · V. Chavagnac · Y. Fouquet

Mineralogy, geochemistry, and Nd isotope composition of the Rainbow hydrothermal field, Mid-Atlantic Ridge

Received: 11 March 2005 / Accepted: 30 November 2005 / Published online: 11 March 2006

Abstract Petrological, geochemical, and Nd isotopic analyses have been carried out on rock samples from the Rainbow vent field to assess the evolution of the hydrothermal system. The Rainbow vent field is an ultramafic-hosted hydrothermal system located on the Mid-Atlantic Ridge characterized by vigorous high-temperature venting (~365°C) and unique chemical composition of fluids: high chlorinity, low pH and very high Fe, and rare earth element (REE) contents (Douville et al., *Chemical Geology* 184:37–48, 2002). Serpentinization has occurred under a low-temperature (<270°C) retrograde regime, later overprinted by a higher temperature sulfide mineralization event. Retrograde serpentinization reactions alone cannot reproduce the reported heat and specific chemical features of Rainbow hydrothermal fluids. The following units were identified within the deposit: (1) nonmineralized serpentinite, (2) mineralized serpentinite—stockwork, (3) steatite, (4) semimassive sulfides, and (5) massive sulfides, which include Cu-rich massive sulfides (up to 28wt% Cu) and Zn-rich massive sulfide chimneys (up to 5wt% Zn). Sulfide mineralization has produced significant changes in the sulfide-bearing rocks including enrichment in transition metals (Cu, Zn, Fe, and Co) and light REE, increase in the Co/Ni ratios comparable to those of mafic Cu-rich volcanic-hosted massive sulfide deposits and different $^{143}Nd/^{144}Nd$ isotope ratios. Vent fluid chemistry data are indicative of acidic, reducing, and high temperature conditions at the subseafloor reaction zone where fluids undergo phase separation most likely under subcritical conditions (boiling). An explanation for the high chlorinity is not straightforward unless mixing with high salinity brine or direct contribution from a magmatic Cl-rich aqueous fluid is considered. This study adds new data, which, combined with the current knowledge of the Rainbow vent field, brings compelling evidence for the presence, at depth, of a magmatic body, most likely gabbroic, which provides heat and metals to the system. Co/Ni ratios proved to be good tools used to discriminate between rock units, degree of sulfide mineralization, and positioning within the hydrothermal system. Deeper units have Co/Ni <1 and subsurface and surface units have Co/Ni >1.

Keywords Massive sulfides · Serpentinite · Nd isotopes · Mid-Atlantic Ridge · Rainbow vent field

Editorial handling: B. Lehmann

A. F. A. Marques (✉) · F. Barriga
CREMINER/Departamento de Geologia,
Faculdade de Ciências, Universidade de Lisboa,
Edifício C6, Piso 4, Campo Grande,
Lisboa 1749-016, Portugal
e-mail: afamarques@fc.ul.pt
Tel.: +351-21-7500000
Fax: +351-21-7500064

V. Chavagnac
National Oceanography Centre,
Southampton, European Way,
Southampton SO14 3ZH, UK

Y. Fouquet
IFREMER, Centre de Brest,
Plouzané BP 70,
Plouzané 29280, France

Introduction

More than 100 hydrothermal sites were discovered over the past 25 years along the worldwide network of mid-ocean ridges (Baker and German 2004). Most hydrothermal sites are basalt-hosted with seafloor venting corresponding to the visible part of a complex and vigorous fluid circulation system active at the subsurface. A typical modern seafloor sulfide deposit encompasses a consolidated sulfide mound underlain by a subseafloor stockwork and covered by active and inactive chimney structures, hydrothermal crusts, metalliferous sediments, and sulfide debris (Goodfellow and Franklin 1993; Fouquet et al. 1993a,b, 1996; Rona et al. 1993; Alt 1995; Hannington et al. 1995; Herzig and Hannington 1995; Humphris et al. 1995). These features commonly found in modern seafloor deposits correlate well with those of ancient volcanic-hosted massive sulfide (VMS) deposits (Doyle and Allen 2003). Both ancient ore-

grade VMS deposits and their modern analogs result from subseafloor heat-driven seawater circulation reacting with crustal or upper mantle rocks and producing syngenetic accumulations of massive sulfides hosted by submarine volcanic successions (Large 1992 and references therein; Barrie and Hannington 1997).

There is a strong relation between the base metal contents in VMS deposits and the nature of their host rocks (Barrie and Hannington 1997). In accordance to this, VMS deposits (ancient and modern) can be divided into five categories: (1) mafic, (2) bimodal-mafic, (3) mafic-siliciclastic, (4) bimodal-felsic, and (5) bimodal-siliciclastic. Mafic VMS deposits are smaller, Cu-rich and Pb-poor deposits are generally associated with synvolcanic intrusions considered to be the heat and metal sources (Barrie and Hannington 1997). Several modern seafloor sulfide deposits along the Mid-Atlantic Ridge (MAR) (e.g., TAG, MESO, Snake Pit) have characteristics comparable to those of mafic VMS deposits in which sediment-starved, high temperature deposits are Cu- and Co-rich with high Cu/Zn ratios contrasting with lower temperature sedimented ridges that are Zn- and Pb-rich (Kase et al. 1990; German et al. 1993; Fouquet et al. 1993a,b; Goodfellow and Franklin 1993; Rona et al. 1993; Tivey et al. 1995; Langmuir et al. 1997; Herzig et al. 1998; Münch et al. 1999; Charlou et al. 2000; Lawrie and Miller 2000; Douville et al. 2002). Although in mafic rocks Ni is in excess relative to Co, the related VMS hold Co-rich sulfides most likely due to the more chalcophile behavior of Co (Hawley and Nichol 1961).

The recent discovery of ultramafic-hosted seafloor hydrothermal systems at the MAR adds a new perspective to the dynamics of seafloor hydrothermal processes and the influence of host rocks. So far there are five known ultramafic-hosted hydrothermal sites at the MAR: Rainbow, Logatchev, Lost City, Saldanha, and Menez Hom, which are all linked to serpentinization reactions and high methane anomalies (Batuyev et al. 1994; German et al. 1996; Donval et al. 1997; FLORES Cruise Report 1998; IRIS Cruise Report 2001; Kelley et al. 2001; SEAHMA Cruise Report 2003). Rainbow and Logatchev are vigorous high-temperature systems with high bulk Cu/Zn ratios, high Cu and Co, and low Pb producing metal-rich black smoker fluids while Saldanha and Menez Hom are low temperature diffuse systems (<10°C) (Batuyev et al. 1994; Bogdanov et al. 1995; Lein et al. 2001; IRIS Cruise Report 2001; Douville et al. 2002; SEAHMA Cruise Report 2003; Marques, Ph.D. thesis in preparation). The Lost City field contains carbonate–brucite chimneys venting high pH fluids (pH 9–10) at intermediate temperatures (40–75°C) (Kelley et al. 2001; Früh-Green et al. 2003; Allen and Seyfried 2004). Serpentinization-driven hydrothermalism seems to be the leading process occurring at Lost City, Saldanha, and Menez Hom (Barriga et al. 1998, 2004; Kelley et al. 2001; Früh-Green et al. 2003; Allen and Seyfried 2004; Costa 2005).

The Rainbow hydrothermal vent field is a vigorous hydrothermal system hosted in completely serpentinized peridotites. Rainbow vent fluids are characterized by the highest temperature reported for MAR fluids (365°C), the highest chloride concentration (750 mM), the lowest end-member pH (2.8), high trace metal contents (Fe, Cu, Zn, Co, and Ni), and high REE and K, Rb, and Cs contents (Douville et al. 2002). These unique physical and chemical characteristics have raised numerous questions concerning the processes acting at Rainbow. Recent cruises at the Rainbow hydrothermal vent field (e.g., HEAT cruise 1994, FLORES cruise 1998, and IRIS cruise 2001) have enabled a thorough understanding of its tectonic setting, hydrothermal fluid and particle chemistry, and record of hydrothermal activity by sediment coring (German et al. 1996; Barriga et al. 1997; Donval et al. 1997; Douville et al. 1997, 2002; Parson et al. 1997; Gràcia et al. 2000; Cave et al. 2002; Edmonds and German 2004; Chavagnac et al. 2005). However, our knowledge of the subsurface structure of the Rainbow active hydrothermal system remains very limited. Fluid interaction and mineralization processes need to be addressed to reach a better understanding of the function of this ultramafic-hosted hydrothermal system.

In this paper, we present a detailed, comprehensive, and thorough description of the geological setting, structure, and mineralogy of the Rainbow hydrothermal sulfide deposit and underlying stockwork from the rock precursor serpentinite to massive sulfides. The field data and sampling result not only from the cruises mentioned before but also, and mainly, from the SALDANHA (1998), IRIS (2001), and SEAHMA (2002) cruises (IRIS Cruise Report 2001; SALDANHA Cruise Report 1999; SEAHMA Cruise Report 2003). We have carried out geochemical and Nd isotope analyses to characterize the Rainbow hydrothermal deposit and to assess the evolution of its formation.

Geological setting

The Rainbow hydrothermal vent field is located on the MAR at the inside corner of a nontransform offset, which links the second-order ridge segments ALVIN MAR (AMAR) and South AMAR (36°14′N; 33°53′W) (Fig. 1). The vent area is composed of a group of at least ten black smokers

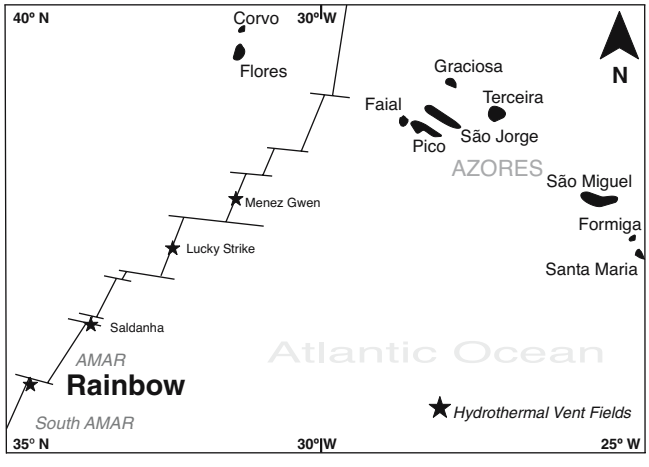

Fig. 1 Location of the Rainbow vent field in a nontransform offset between the AMAR and South AMAR second-order segments at the MAR, south of the Azores Islands

expelling high-temperature (~365°C) fluids with evidence of phase separation at depth (Fouquet et al. 1997; Douville et al. 2002).

Field observations during remotely operated vehicle (ROV) dives and IRIS and SEAHMA cruises coupled with sample location data collected during the SEAHMA, IRIS, and FLORES cruises have enabled the drafting of a detailed geological map of the vent field area (Fig. 2a) (FLORES Cruise Report 1998; SEAHMA Cruise Report 2003; IRIS Cruise Report 2001). In the Rainbow ridge area, completely serpentinized peridotite outcrops covered by whitish pelagic sediment are often crosscut by normal faults exposing the serpentinite. On the western limit of the active vent area, a subvertical normal fault trending N–S reveals ultramafic rocks with visible networks of sulfide-bearing veinlets (i.e., a well-defined stockwork). In the upper part of the scarp, sulfides become more abundant occurring as semimassive sulfides. The active venting area contains numerous active and inactive sulfide chimneys that lie on top of sulfide mounds built up mostly by the accumulation of collapsed, dead chimneys. Basalt outcrops were found exclusively on the bottom of the South AMAR segment (W of Rainbow ridge) and at the easternmost section of the vent field area at the summit of the Rainbow ridge. The basalts at the ridge summit are pillow lavas and overlie the serpentinites. So far, no contact was recognized (FLORES Cruise Report 1998). Figure 2b shows a geological profile which combines bathymetry with sample type and location (SEAHMA cruise) and ROV observations (SEAHMA cruise).

Sample description

From the rock suite collected during the IRIS and SEAHMA cruises using ROV and dredges, 128 samples were selected. Among these, 71 were carefully studied under transmitted and reflected light microscopy. Figure 3 illustrates a paragenetic sequence in the Rainbow rocks and ores and Fig. 4 contains thin section microphotographs taken from representative samples of the ore deposit.

Host rocks

Serpentinites (Srp) that form the substratum of the Rainbow vent field are nondeformed and comprise serpentine-group minerals (mainly lizardite) with well-preserved

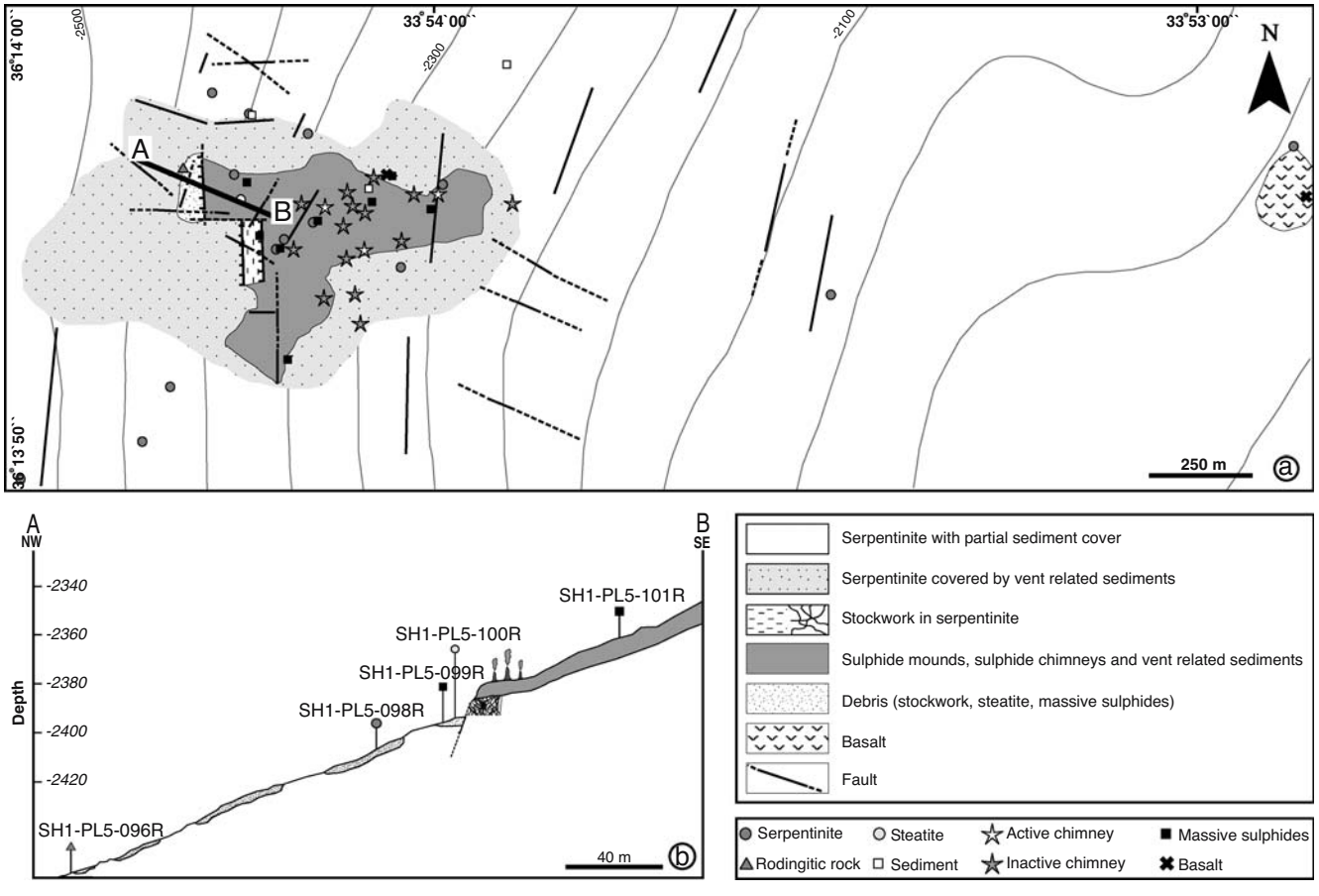

Fig. 2 **a** Geological map of the Rainbow vent field area with sample location (geology and sample location from direct observations during IRIS and SEAHMA1 cruises and FLORES cruise report; bathymetric data and ADELIE software from IFREMER). *Line AB* is the cross-section represented in subpanel b. **b** Interpretative geological cross-section with no vertical exaggeration, representing location of samples collected during dive SH1-PL5 of the SEAHMA1 cruise

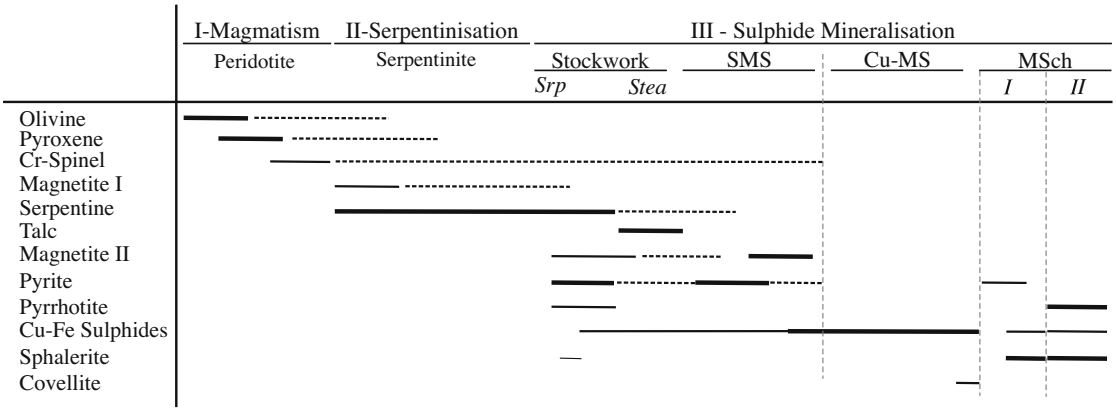

Fig. 3 Paragenetic sequence of minerals present in studied rocks from the Rainbow vent field. Increasing mineral abundances are represented by increasing line thickness. *Srp* Serpentinite, *Stea* steatite, *SMS* semimassive sulfides, *Cu-MS* Cu-massive sulfides, *MS ch* massive sulfide chimneys

pseudomorphic textures (mesh, hourglass, and bastite), dust-like euhedral grains of magnetite (mgt) I and accessory anhedral Cr-spinel with hydrothermally altered rims (Fig. 4a, b). These features correspond to serpentinites that resulted from simple peridotite-seawater interactions under static, low-temperature, and retrograde metamorphism. Subsequent, sigmoidal cross-fractures filled with fibrous γ-serpentine and carbonate-filled veins define the late and brittle deformation stage.

Sulfide-bearing zones

Progressive percolation of high-temperature mineralizing hydrothermal fluids through the serpentinite induced the pervasive replacement of silicate mineralogical assemblages resulting in textural changes (Fig. 4c–h). The various sulfide-bearing rocks are described below:

Stockwork in serpentinite (St)

Pseudomorphic serpentine-group minerals that are characteristic of serpentinites are replaced by nonpseudomorphic featureless serpentine, mainly chrysotile (Fig. 4c). The earliest hydrothermal sulfides occur here, either disseminated or in veinlets and surrounded by the nonpseudomorphic serpentine matrix. Euhedral to anhedral pyrite (py) grains are ubiquitous and predate all other sulfide phases. Intermediate solid solution sulfides with exsolved chalcopyrite (ISS/Ccp) occur mostly as spherical aggregates or small anhedral grains dispersed within the serpentine matrix and occasionally replace py. Sometimes fine-grained covellite occurs as rims surrounding ISS/Ccp. Euhedral lamellar crystals of pyrrhotite (po) and sometimes sphalerite (sp) may occur. Dust-like mgt I produced during serpentinization disappears and a new, coarse-grained mgt II indicative of late oxidizing conditions occur as individual and dispersed grains that often replace py. Hydrothermally altered Cr-spinel relics (Cr-spl) reveal highly reflective borders of "ferritchromit." Large, euhedral, and radial prisms of aragonite occur along veins previously filled by sulfides.

Steatite (Stea)

Locally, stockwork serpentinites with incipient sulfide mineralization have undergone a different type of hydrothermal alteration where talc has extensively replaced serpentine-group minerals forming steatite (soapstone) (Fig. 4d). Oxides like mgt are rare and relic Cr-spl grains are highly altered. Trace sulfides may occur. Usually po associated with ISS/Ccp and, more rarely, with altered py.

Semi-massive sulfides (SMS)

The semimassive sulfide unit is the result of the pervasive replacement of stockwork silicates by hydrothermal sulfides. Here, host rock relics may be preserved as extremely altered serpentinite "islands" surrounded by sulfide masses or as altered Cr-spl relics that prove the ultramafic nature of the host rock (Fig. 4e). Sulfide assemblages are similar to the ones observed in stockwork samples. Anhedral masses of py are sometimes replaced by mgt II or by ISS/Ccp.

Massive sulfides (MS)

Cu-massive sulfides (Cu-MS) Cu-massive sulfides are characterized by a dense array of ISS/Ccp sulfides with low porosity and no apparent mineralogical zonation. This unit results from extensive replacement of the py-rich semimassive sulfide ore by ISS/Ccp. Some sections show annealing (120° joints) indicative of recrystallization processes (Fig. 4f). ISS/Ccp contains altered rims of covellite and rare fracture-filling anhydrite.

Massive sulfide chimneys (MS-ch I, II) As opposed to Cu-MS, sulfide chimneys are porous and frequently

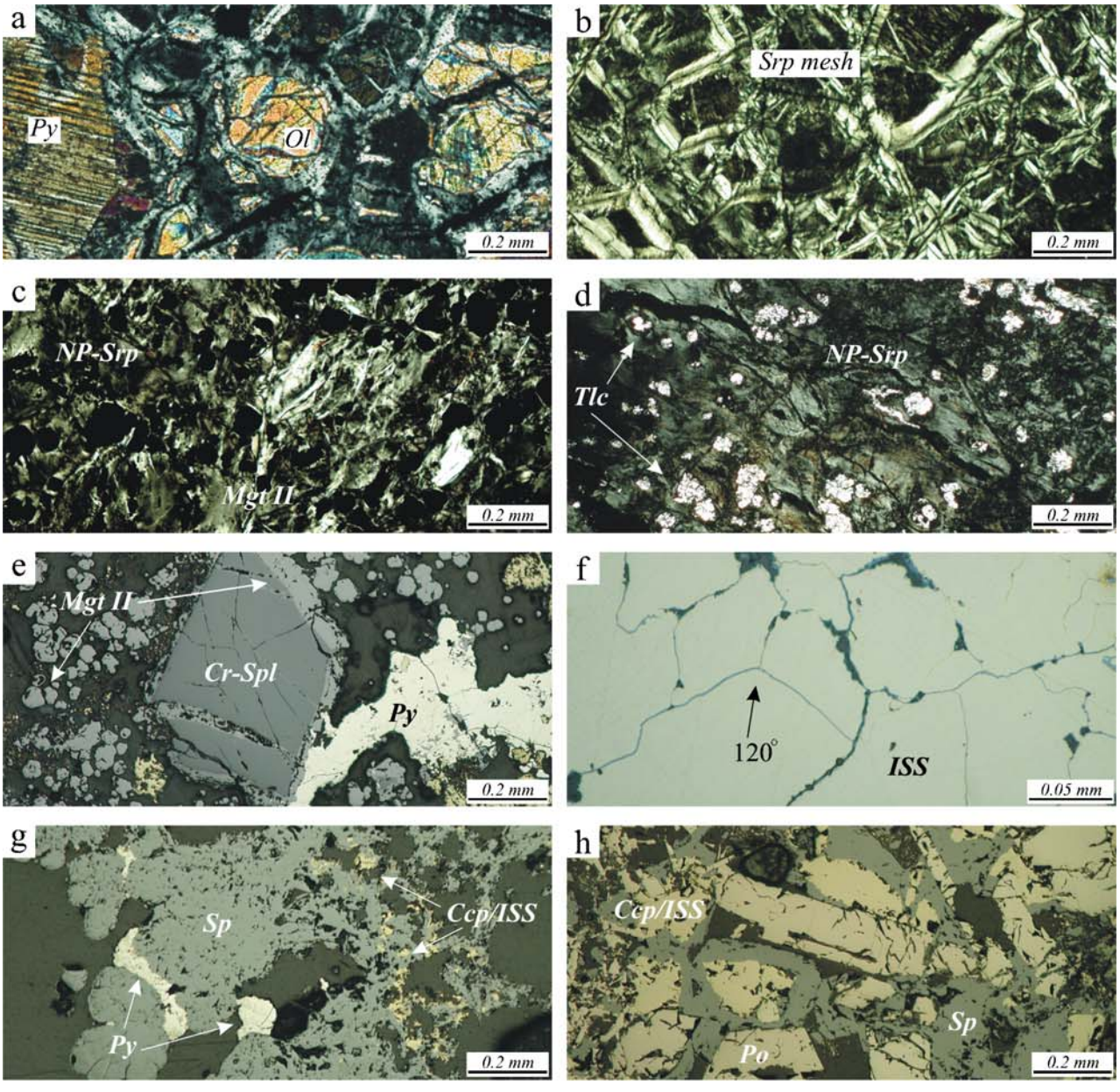
a
Py
Ol
0.2 mm
b
Srp mesh
0.2 mm
c
NP-Srp
Mgt II
0.2 mm
d
NP-Srp
Tlc
0.2 mm
e
Mgt II
Cr-Spl
Py
0.2 mm
f
120°
ISS
0.05 mm
g
Sp
Ccp/ISS
Py
0.2 mm
h
Ccp/ISS
Sp
Po
0.2 mm

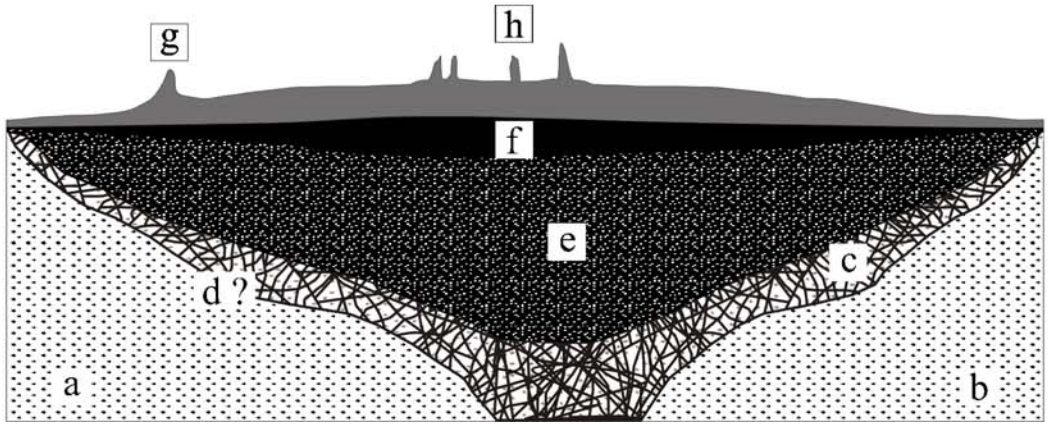
g
h
f
e
c
d ?
a
b

◀ **Fig. 4** Interpretative scheme through the active area of Rainbow vent field. Microphotographs taken under reflected light, except subpanels a, b, c, and d taken with transmitted light with crossed nicols. **a** Partially serpentinized peridotite with pyroxene, olivine, and serpentine mesh (after olivine). **b** Serpentinite with well-developed serpentine mesh texture after olivine. **c** Mineralized serpentinite (stockwork) with nonpseudomorphic featureless serpentine and coarse-grained magnetite II. **d** Transitional stage between stockwork and steatite where the nonpseudomorphic serpentine is gradually replaced by talc. **e** Semimassive sulfide unit (SMS) with relics from the rock precursor (Cr-spinel and highly altered phyllosilicates). **f** Recrystallized Cu-rich massive sulfide unit (Cu-MS) with intermediate solid solution/chalcopyrite exhibiting 120° jointing. **g** Massive sulfide chimney (*type I*) with low temperature sulfide assemblage pyrite + Zn-sphalerite + chalcopyrite/intermediate solid solution. **h** Massive sulfide chimney (*type II*) with high temperature sulfide assemblage, pyrrhotite + Fe-sphalerite + intermediate solid solution/chalcopyrite. *Ccp/ISS* Exsolved chalcopyrite in intermediate solid solution, *Cr-spl* Cr-spinel, *ISS* intermediate solid solution, *Mgt II* magnetite II, *NP-srp* nonpseudomorphic serpentine, *Ol* olivine, *Po* pyrrhotite, *Px* pyroxene, *Py* pyrite, *Sp* sphalerite, *Srp mesh* serpentine with mesh texture, *Tlc* talc

show concentric mineralogical zonation around a vent orifice. Textures correspond to an interlocking network of sulfides representative of open-space type deposition due to mixing of a hot metal-rich vent fluid with cool seawater. Rainbow hydrothermal chimneys are sp-rich (Fig. 4g,h). MS-ch type I are defined by a lower temperature sulfide assemblage composed of euhedral py overprinted by colloform sp with ISS/Ccp intergrowths (Fig. 4g). MS-ch type II contain lamellar crystals of po interlocked with sulfide aggregates. The latter are zoned with an ISS/Ccp core rimmed by chalcopyrite both surrounded by colloform sp (Fig. 4h). Textural evaluation of MS-ch type II indicates cogenetic sulfide formation and assemblages that are compatible with high temperature venting.

Rodingitic rocks

A few samples are composed of relics of extremely altered rodingite-like, serpentinized material in a matrix of aragonite, which appears to have extensively replaced former serpentinites. Petrography reveals aggregates of interpenetrating serpentine with rare bastite relics plus chlorite and rare garnet (grossular/hydrogrossular) surrounded by euhedral grains of aragonite. Large hydrothermal diopside grains that are not in textural equilibrium with aragonite may overprint the serpentine/chlorite aggregates. These assemblages are indicative of Ca mobilization after retrograde serpentinization somewhat similar to the rodingitization processes as described by O'Hanley (1996).

Methodology

Electron microprobe analyses were performed using a CAMECA SX50 with three crystal spectrometers at the University of Toronto. Silicates were analyzed using an accelerating voltage of 15 kV and sample current of 15 nA with a beam diameter of 3 μm. The sulfide and oxide routine took place under an accelerating voltage of 20 kV and sample current of 30 nA with a beam diameter of 1 μm. A few serpentine-group minerals were analyzed at the University of Lisbon using a JEOL JCXA 733 microprobe. Whole-rock geochemistry analyses were undertaken by ACTLABS, Canada using the LITORESEARCH QUANT package. The procedure for the rock pulverization were as follows: (1) selected samples were diamond-sawn into small slices (<1.5 cm thick), (2) slices were then ground using a diamond-grinding wheel to prevent contamination, (3) then samples were carefully washed and dried at 25°C, (4) dried samples were crushed using a hammer while enclosed within thick paper envelopes to prevent metal contamination, and (5) small fragments were then powdered in an agate ring mill. For Nd isotope analyses, 100 mg to a few grams of bulk powder samples were dissolved either in a mixture of HCl and HNO_3, or HF and HNO_3 in a 3:1 proportion followed by a second step in concentrated HNO_3 in a sealed savillex beaker and left on a hotplate at 150°C for a couple of days. The solution was then dried and converted to chloride form by adding 5 to 10 ml of 6 M HCl. Separation of Sm and Nd was done using a routine two column ion-exchange technique, which first extracts REE through a cation exchange column followed by a separation of Nd from Sm through a second column packed with Kel-F Teflon-coated HDEHP. Nd isotope ratios were measured at the National Oceanography Centre, Southampton, England on a seven-collector VG Sector 54 mass spectrometer. The $^{143}Nd/^{144}Nd$ ratios were determined in multidynamic collection mode. Isotope ratios were normalized to $^{146}Nd/^{144}Nd=0.7219$. Measured values for JNd-i standards were $^{143}Nd/^{144}Nd=0.512104\pm10$ (2 SD, n=38).

Results

Rock sample locations and descriptions of representative samples are reported in Table 1. Results for REE, mineral chemistry, and Nd isotopic compositions are given in Tables 2, 3, and 4, respectively.

Bulk-rock geochemistry

Figure 5 illustrates major and trace element variation of 15 selected samples that represent the mineralizing sequence from serpentinite to massive sulfides.

SiO_2 and MgO contents decrease from serpentinites toward stockwork, semimassive sulfides, and massive sulfides due to gradual silicate destruction with progressive sulfide replacement. Steatites are more silica-rich due to the predominance of talc. Steatites are, at least locally, indicative of higher silica activity and high fluid/rock ratio. Co abundances in the unmineralized serpentinites are below 100 ppm while Co contents in mineralized samples increase with the amount of sulfide mineralization, reaching high concentrations in semimassive sulfides (~2,335 ppm Co, n=4), Cu-MS (~4,770 ppm Co), and MS-ch (6,300 ppm

Table 1 Sample location chart with mineralogy and rock type description

Sample	Dredge start		Dredge finish		Mineralogy	Rock type
	Lat	Lon	Lat	Lon		
IR-DR-01-A-05	36°19.2′N	33°54′W	36°16.2′N	33°45′W	(Ol), (Px), (Spl), Srp, Chl, Mgt	Serpentinite
IR-DR-02-B-04	36°16.2′N	33°54′W	36°13.8′N	33°45′W	(Spl), Srp, Chl, Mgt	Serpentinite
IR-DR-02-D	36°16.2′N	33°54′W	36°13.8′N	33°45′W	(Spl), Srp, Mgt, Py	Stockwork
IR-DR-03-F	36°13.8′N	33°54′W	36°11.4′N	33°45′W	(Spl), Srp, Mgt, Arg	Stockwork
IR-DR-02-C-01	36°16.2′N	33°54′W	36°13.8N	33°45′W	(Spl), Srp, Mgt, Py, ISS/Ccp, Po, Sp, Arg	Stockwork
SH1-DR3-9-4	36°13.8′N	33°54.6′W	36°13.8′N	33°53.4′W	Py, ISS/Ccp, Mgt	Stockwork
SH1-DR3-9-9	36°13.8′N	33°54.6′W	36°13.8′N	33°53.4′W	Py, ISS/Ccp, Mgt	Stockwork
IR-DR-03-E	36°13.8′N	33°54′W	36°11.4′N	33°45′W	(Spl), Tlc, Mgt, Po, ISS/Ccp	Steatite
SH1-DR3-8-3	36°13.8′N	33°54.6′W	36°13.8′N	33°53.4′W	(Spl), Tlc, Mgt, Po, ISS/Ccp	Steatite
IR-DR-01-C-01	36°19.2′N	33°54′W	36°16.2′N	33°45′W	Py, ISS/Ccp, Mgt	Semi-massive sulfide
IR-DR-01-G-02	36°19.2′N	33°54′W	36°16.2′N	33°45′W	(Spl), Py, ISS/Ccp, Mgt	Semi-massive sulfide
SH1-DR3-2-1	36°13.8′N	33°54.6′W	36°13.8′N	33°53.4′W	Py, ISS/Ccp, Mgt	Semi-massive sulfide
SH1-DR3-2-3	36°13.8′N	33°54.6′W	36°13.8′N	33°53.4′W	Py, ISS/Ccp, Po	Semi-massive sulfide
SH1-DR3-1-2	36°13.8′N	33°54.6′W	36°13.8′N	33°53.4′W	ISS/Ccp, Anh	Cu-massive sulfide
IR-DR-02-L-01	36°16.2′N	33°54′W	36°13.8N	33°45′W	Srp, Chl, Arg, Di, Po	Rodingitic material

( ) Relics, *Anh* anhydrite, *Arg* aragonite, *Chl* chlorite, *Di* diopside, *ISS/Ccp* exsolved chalcopyrite in intermediate solid solution, *Mgt* magnetite, *Ol* olivine, *Po* pyrrhotite, *Px* pyroxene, *Py* pyrite, *Sp* sphalerite, *Spl* Cr-spinel, *Srp* serpentine-group minerals, and *Tlc* talc

Co) (Marques, Ph.D. thesis in preparation). Ni is absent in Cu-rich massive sulfides and MS-ch. Unmineralized serpentinites are Cu-depleted (~95 ppm, *n*=7) and Cu abundances remain fairly low in the stockwork (~1,421 ppm, *n*=7) and in steatites (~257 ppm, *n*=3) (Marques, Ph.D. thesis in preparation). In more mineralized rocks, Cu increases sharply and becomes a major element in semimassive sulfides (~11.3wt%, *n*=4), Cu-rich massive sulfides (27.98wt%, *n*=1), and MS-ch (8.35wt%, *n*=1). Selenium is exclusively present in the samples highly enriched in Cu. The high Cu-values are representative of all the strongly mineralized samples, thus, if Rainbow was on land it would be a high-grade copper deposit. Serpentinized peridotites are Ni-rich with lower Co (~1,681 ppm Ni, ~108 ppm Co, *n*=7) and Co/Ni ratios ~0.06 (Marques, Ph.D. thesis in preparation) matching *P*-mantle values (McDonough and Sun 1995). With the development of sulfide mineralization, bulk-rock Co/Ni ratios increase, resulting in stockwork semimassive and massive sulfides with Co/Ni >1 (Fig. 3). In absolute terms, Ni contents in serpentinite and stockwork decrease while Co increases sharply. The peridotite precursor has high Ni and low Co, therefore, it is difficult to explain the final Co/Ni ratios and the extreme Co enrichment in the massive sulfides as resulting solely from an ultramafic source. Zn is absent in most serpentinites and Zn concentrations are rather low with irregular distribution except in Zn-rich chimneys. Sphalerite is the only Zn sulfide found in the Rainbow assemblages, thus, its presence or absence dictates Zn abundances (Fig. 5).

Zn-rich rocks are characteristic of MS-ch (type I and II) and relate to the focused venting at surface where cooler seawater interacts with hotter vent fluid. Chimneys may contain up to 5.12wt% Zn (e.g., Ms-ch II) (Marques, Ph.D. thesis in preparation). On the contrary, Cu-rich rocks show evidences of subseafloor precipitation and recrystallization (Cu-MS) where higher temperatures can be attained. The presence, in these amounts, of Cu, Zn, and Co is characteristic of mafic-hosted seafloor hydrothermal systems. One may expect the contribution of a mafic metal source responsible for Cu, Zn, and Co input along with Fe into the system.

REE concentrations measured in representative rock samples are listed in Table 2. Chondrite-normalized REE patterns are plotted in Fig. 6. With one exception, europium anomalies (Eu/Eu*) are higher than in seawater but still below those of the vent fluid (Fig. 5). Except for three samples, most of the mineralized rocks display relevant positive Eu anomalies (1.22 to 9.15), suggesting interaction with hydrothermal fluids. Serpentinites, stockwork, and steatites present flat heavy REE (HREE) normalized values at about chondrite abundances. Serpentinites show a nearly flat LREE pattern parallel to seawater with a weak Ce negative anomaly (Fig. 6a). Stockwork samples depict LREE enrichment over HREE, somewhat comparable to vent fluid REE patterns with a slight negative Ce anomaly (Fig. 6b). REE patterns of semimassive sulfides clearly reflect the vent fluid REE pattern with significant LREE enrichment and positive Eu anomalies. Cu-rich massive sulfides are REE-depleted (Fig. 6d). Steatite and rodingitic material show LREE patterns similar to stockwork but with no Ce anomaly (Fig. 6c).

Mineral chemistry

Four hundred thirty-eight microprobe analyses were completed where 308 are in sulfides. Chemical compositions of py, po, ISS/Ccp, and sp from the different rock types are reported in Table 3.

Table 2 Rare earth element (REE) analysis (in ppm) of serpentinites, stockwork, steatites, rodingitic material, semimassive sulfides, and massive sulfides from the Rainbow vent field

Sample type	IR-DR-01-A-05	IR-DR-02-B-04	IR-DR-02-D	IR-DR-03-F	IR-DR-02-C	SH1DR3-9-4	SH1DR3-9-9	SH1DR3-2-3	SH1DR3-2-1	IR-DR-01-C-01	IR-DR-01-G-02	SH1DR 3-1-2	SH1DR 3-8-3	IR-DR-03-E	IR-DR-02-L-01	BIR-1	BIR-1	DNC-1	DNC-1
	Serp	Serp	St	St	St	St	St	SMS	SMS	SMS	SMS	Cu–MS	Stea	Stea	Rod	Measured	Certified	Measured	Certified
La	1.03	0.07	1.10	1.03	0.21	2.08	1.39	7.36	21.46	19.23	2.39	0.21	2.13	0.48	0.64	0.81	0.62	3.91	3.8
Ce	1.46	0.09	0.80	0.73	0.33	1.50	1.39	7.80	20.27	21.27	2.66	0.43	2.17	0.45	1.18	2.11	1.95	8.59	10.6
Pr	0.28	0.01	0.11	0.12	0.03	0.20	0.16	0.56	1.23	1.47	0.19	0.05	0.15	0.04	0.12	0.39	0.38	1.04	1.3
Nd	0.93	<0.05	0.30	0.27	0.13	0.52	0.44	1.78	3.54	4.54	0.57	0.16	0.45	0.11	0.47	2.52	2.5	4.95	4.9
Sm	0.21	0.01	0.05	0.05	0.04	0.08	0.09	0.28	0.44	0.60	0.07	0.03	0.07	0.03	0.11	1.13	1.1	1.43	1.38
Eu	0.09	0.01	0.04	0.03	0.01	0.26	0.03	0.1	0.81	0.05	0.03	0.01	0.01	0.02	0.11	0.55	0.54	0.62	0.59
Gd	0.25	<0.01	0.08	0.05	0.03	0.09	0.09	0.18	0.32	0.36	0.05	0.02	0.05	0.04	0.15	1.86	1.85	2.05	2
Tb	0.04	<0.01	0.01	<0.01	<0.01	<0.01	<0.01	0.02	0.06	0.05	<0.01	<0.01	<0.01	0.01	0.03	0.39	0.36	0.41	0.41
Dy	0.26	0.01	0.08	0.04	0.04	0.07	0.07	0.09	0.29	0.16	0.02	0.02	0.05	0.06	0.18	2.65	2.5	2.73	2.7
Ho	0.06	<0.01	0.02	<0.01	<0.01	<0.01	<0.01	0.01	0.06	0.02	<0.01	<0.01	<0.01	0.01	0.04	0.55	0.57	0.59	0.62
Er	0.18	0.01	0.05	0.02	0.02	0.05	0.05	0.02	0.17	0.04	<0.01	0.01	0.04	0.05	0.13	1.84	1.7	2.02	2
Tm	0.03	<0.005	0.01	<0.005	<0.005	<0.005	0.005	<0.005	0.02	<0.005	<0.005	<0.005	0.05	0.01	0.02	0.29	0.26	0.32	(0.33)
Yb	0.18	0.03	0.05	0.02	0.04	0.02	0.03	0.01	0.13	0.02	<0.01	<0.01	0.03	0.05	0.13	1.65	1.65	1.93	2.01
Lu	0.03	0.004	0.01	0.004	0.005	0.004	0.005	0.003	0.02	<0.002	<0.002	<0.002	0.01	0.01	0.02	0.26	0.26	0.31	0.32
$(Eu/Eu^*)_N$	1.17	-	1.88	1.83	1.22	9.15	0.88	1.32	6.55	0.35	1.47	1.44	0.26	1.85	2.52				
$(Ce/Ce^*)_N$	0.75	0.99	0.49	0.48	0.93	0.49	0.66	0.73	0.67	0.76	0.77	1.13	0.71	0.65	1.03				
$(La/Yb)_N$	3.89	1.59	14.95	34.99	3.79	58.7	29.11	351.5	108.6	650.5	–	–	47.53	6.52	3.34				

n.d. Not detected

Table 3 Electron microprobe analyses (average values in wt%) of pyrite, pyrrhotite, ISS/Ccp, and sphalerite from the Rainbow vent field

Mineral	Lithology		Fe	Cu	S	Ag	Zn	Cd	Ni	Co	Total	N
Pyrite	Early stockwork		43.6	–	50.5	–	–	–	3.46	0.10	97.8	3
	Stockwork		46.3	–	52.9	–	0.01	–	0.32	0.03	99.5	34
	Steatite		46.2	0.01	53.2	0.01	0.01	–	0.02	0.20	99.6	8
	SMS		46.4	0.10	53.3	0.01	0.04	0.01	0.03	0.18	100.1	45
	MSch I		45.3	–	52.5	–	0.30	–	–	0.12	98.26	4
Pyrrhotite	Stockwork		59.7	0.01	39.4	0.01	0.03	0.03	0.38	0.04	99.58	19
	Steatite		59.8	0.11	38.6	0.01	0.02	0.02	0.10	0.33	99.04	8
	SMS		60.9	0.02	38.4	0.02	0.02	0.03	0.11	0.06	99.55	24
	MSch II		59.6	0.02	38.8	0.02	0.19	0.02	0.01	0.40	99.09	3
ISS/Ccp	Stockwork	ISS	40.7	22.3	35.7	0.02	0.66	0.03	0.26	0.09	99.71	8
		Ccp	31.0	33.6	35.5	0.03	0.36	0.02	0.13	0.03	100.6	9
	Steatite	ISS	39.7	23.9	35.0	0.01	0.19	0.02	0.05	0.41	98.39	4
		Ccp	32.3	29.9	34.6	0.01	0.21	0.03	0.03	0.22	98.70	3
	SMS	ISS	40.8	20.4	37.7	0.01	0.31	0.03	0.07	0.07	99.39	11
		Ccp	32.3	32.3	35.2	0.01	0.13	0.02	0.04	0.20	100.2	30
	Cu-MS	ISS	39.2	24.7	35.4	0.01	0.03	0.02	0.01	0.52	100.0	13
	MSch I	Ccp	30.8	33.1	34.8	0.02	1.21	0.02	0.01	0.02	99.98	5
	MSch II	ISS	42.2	21.7	36.0	0.03	0.16	0.01	–	0.34	100.4	8
		Ccp	34.5	29.9	35.3	0.07	0.24	0.06	0.02	0.18	100.2	1
Sphalerite	Stockwork	Marm	13.4	0.04	33.7	0.01	52.9	0.11	0.01	0.01	100.2	20
		Sp	3.15	0.05	33.0	0.00	63.2	0.12	0.01	0.00	99.60	10
	MS-ch type I	Marm	10.7	0.90	32.6	0.07	53.5	0.33	–	0.05	98.16	5
		Sp	1.40	0.22	31.8	0.10	62.8	0.06	–	0.01	96.45	5
	MS-ch type II	Marm	15.6	0.36	34.9	0.01	49.7	0.09	–	0.27	99.95	3

N Number of microprobe analyses, – not detected, *SMS* semimassive sulfides, *MSch I-II* massive sulfide chimneys type I and II, *Py* pyrite, *ISS/Ccp* intermediate solid solution with exsolved chalcopyrite lamellae, *Po* Pyrrhotite, *Sp* sphalerite, and *Marm* marmatite

Fe/S ratios in py are fairly constant except in the early stockwork where py is Ni-rich containing up to 3.46wt% Ni and 0.1wt% Co. Figure 7 illustrates the Co and Ni variation in py minerals from the Rainbow vent field. Stockwork contains Ni-rich py whose Ni contents decrease gradually toward the semimassive sulfides and MS-ch. In contrast, low Co concentrations found in stockwork py increase toward the semimassive sulfides and MS-ch. Hence, py from stockwork has Co/Ni <1 and the remaining py from the semimassive sulfides, MS-ch, and steatites are Co-rich with Co/Ni >1. A similar Co/Ni ratio variation is observed for po, ISS/Ccp, and sp with the exception that po from semimassive sulfides still reveals Co/Ni <1.

ISS/Ccp chemistry is complex although comparable to that of the Bent Hill and ODP mounds on the Juan de Fuca Ridge (Lawrie and Miller 2000). Fe and Cu proportions vary widely (Fe ~42.16 to ~30.75wt%, Table 4) due to chalcopyrite exsolution lamellae. These nonstoichiometric concentrations suggest that no equilibrium was attained in the newly formed sulfides. Zn contents in the chalcopyrite portions are variable: ~0.36wt% in St, ~0.13wt% in SMS, ~1.21wt% in MS-ch I, ~0.24wt% in MS-ch II, and 0.21wt%

Table 4 Nd isotope data from representative samples of the Rainbow vent field

Sample	Rock type	Nd (ppm)	1/Nd	$^{143}Nd/^{144}Nd$	±2sE	ε_{Nd}
IR-DR-02-L-01	Rodingitic material	0.47	2.13	0.513030	16	7.65
IR-DR-03-E	Steatite	0.11	9.09	0.513066	53	8.35
SH1-DR3-8-3	Steatite	0.45	2.21	0.513082	16	8.66
IR-DR-01-G-02	Semi-massive sulfide	0.57	1.75	0.513056	8	8.15
IR-DR-01-C-01	Semi-massive sulfide	4.52	0.22	0.513069	8	8.41
SH1-DR3-2-1	Semi-massive sulfide	3.54	0.28	0.513075	6	8.52
SH1-DR3-2-3	Semi-massive sulfide	1.78	0.56	0.513069	9	8.41
SH1-DR3-9-9	Stockwork	–	–	0.513053	15	8.10
SH1-DR3-9-4	Stockwork	0.52	1.91	0.513073	6	8.49
IR-DR-02-C	Stockwork	0.13	8.00	0.513075	55	8.52
IR-DR-03-F	Stockwork	0.30	3.33	0.513025	26	7.55
IR-DR-01-A-05	Serpentinite	0.93	1.08	0.512926	6	5.62

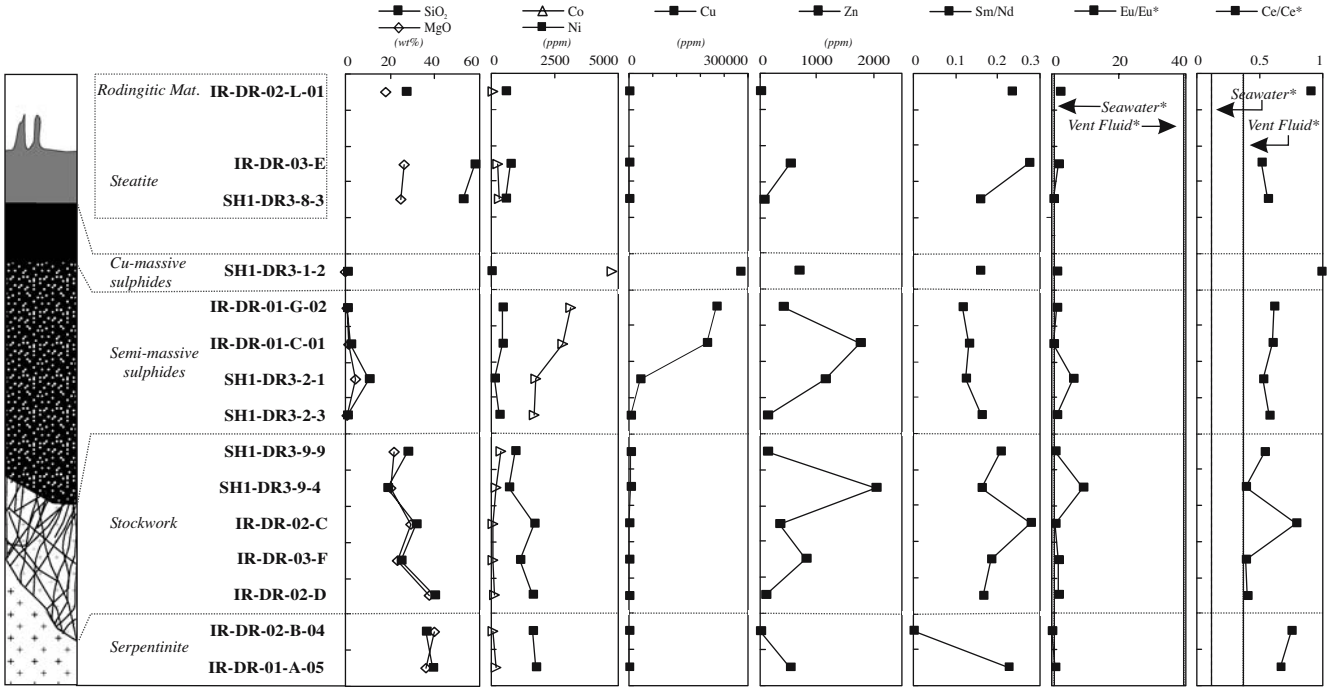

Fig. 5 Bulk-rock chemical data of selected elements (SiO_2, MgO, Co, Ni, Cu, Zn, Sm/Nd, Eu/Eu*, Ce/Ce*) from representative samples of the upper section of the hydrothermal system

in Stea. The same defines the ISS portion, which contains ~0.66wt% in St, ~0.31wt% in SMS, 0.03wt% in Cu-MS, 0.16wt% in MS-ch II, and 0.19wt% in Stea. Experimental work by Kojima and Sugaki (1985) simulating hydrothermal conditions for the Cu-Fe-Zn-S system between 300 and 500°C and pressures of 500 kg/cm^2 confirmed that the Zn content of ISS and chalcopyrite decreases with decreasing temperature as previously observed by Hutchinson and Scott (1981). If we consider either of the main mineralizing sequences, St–SMS–MS-ch II and St–Stea, Zn contents in ISS/Ccp decrease upwards, which suggests a decrease in temperature as is to be expected. This does not apply to Cu-MS and MS-ch I units. The first, which is Zn-free, probably results from recrystallization and zone refining inducing Zn remobilization, whereas Ccp in MS-ch I shows anomalously high Zn contents possibly due to small sp inclusions. Because ISS can easily turn into chalcopyrite, the regular presence of ISS in Rainbow in-

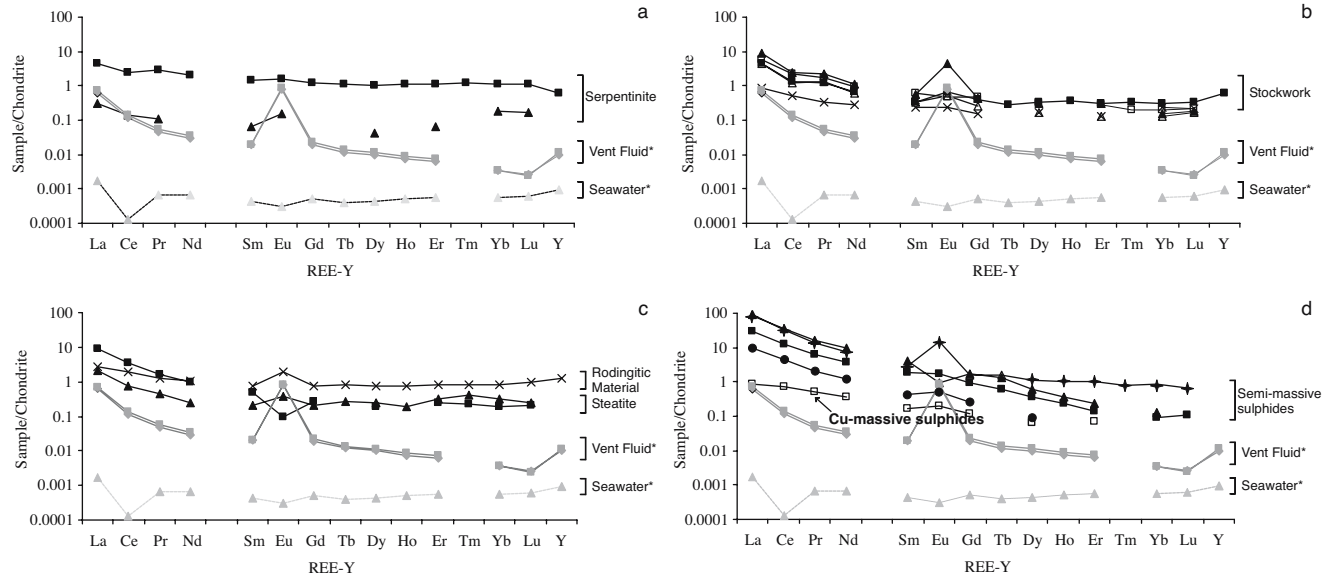

Fig. 6 Chondrite normalized REE patterns for selected representative Rainbow vent field rocks. **a** Serpentinites. **b** Stockwork. **c** Steatite and rodingitic material. **d** semimassive and massive sulfides. Data in Table 3. Normalizing values after McDonough and Sun (1995). *Rainbow vent fluid data (×10) and seawater data (×100) after Douville et al. (2002)

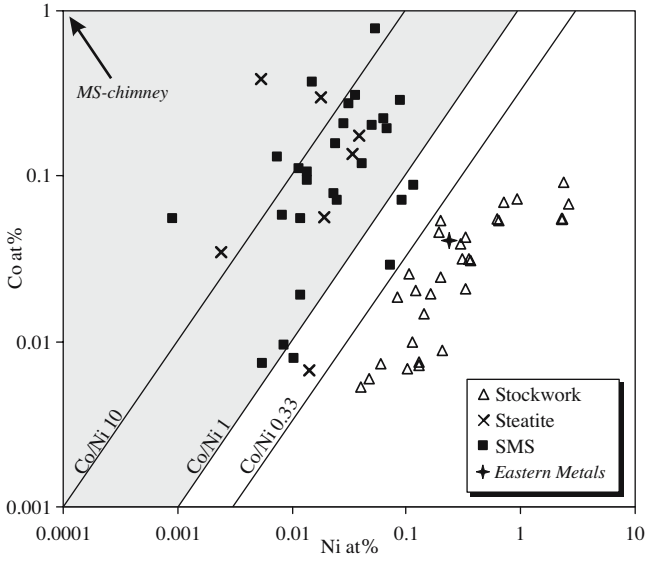

Fig. 7 Co vs Ni (at.%) plot for pyrite from the Rainbow vent field. Pyrite from MS-ch I is not represented because Ni is absent. The *black star* represents the average value of pyrite from the serpentinite-hosted Eastern Metals deposit (Auclair et al. 1993). The compositional field where Co/Ni >1 (*shaded area*) delimits pyrites of volcanogenic association (VMS) (Loftus-Hills and Solomon 1967; Bralia et al. 1979; Mookherjee and Philip 1979; Walshe and Solomon 1981; Bajwah et al. 1987; Lawrie and Miller 2000)

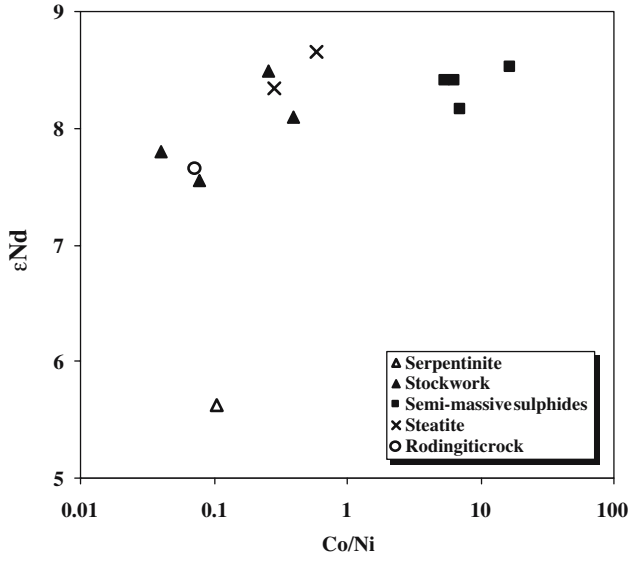

Fig. 8 εNd vs bulk-rock Co/Ni ratios in selected samples from the Rainbow vent field

dicates rapid cooling with effective sealing (Kase et al. 1990). There are two distinct populations of sp according to FeS contents. Lower FeS values (2.9 to 3.4wt% in St and 2.45 to 0.9wt% in MS-ch I) correspond to sp_{ss} associated with py. High FeS values (10.41 to 17.9wt% in St to 14.41 to 17.29wt% in MS-ch II) correspond to sp (marmatite), related to po–ISS/Ccp assemblages. Low FeS in sp suggests increasing sulfur activity (aS_2), decreasing temperature, or the combination of both (Vaughan and Craig 1997). Marmatite (Cu-rich) occurs in MS-ch I associated with ISS/Ccp (Zn-rich), suggesting the presence of minute inclusions of ISS/Ccp within marmatite and interference during analytical processes. Sphalerite specimens from sulfide chimneys contain relevant amounts of Cu, Ag, and Cd (MS-ch I) or Cu and Co (MS-ch type II). Variation in the FeS contents from sp, if in equilibrium with py or po, suggest that their precipitation occurred under different conditions, most probably at different temperatures. This may reflect different degrees of mixing of hotter vent fluid with cold seawater on proximal and distal areas of the hydrothermal system.

Nd isotopes

Radiogenic isotopes are powerful tools for identifying sources and processes and are used in conjunction with trace element data to identify fluid source(s). The Nd isotope compositions of 12 samples from the Rainbow sulfide deposit are reported in Table 4 and plotted against Co/Ni and 1/Nd in Figs. 8 and 9. The high Nd (and REE) concentrations of the semimassive sulfides compared with the other mineralized samples are most probably related to the occurrence of phyllosilicates because REE are not easily incorporated in sulfides. This would also explain the REE-depletion in silicate-free massive sulfides (Table 2).

$^{143}Nd/^{144}Nd$ ratios of all samples, apart from serpentinite, vary in a narrow range between 0.513025 and 0.513082, corresponding to a ε_{Nd} of +7.55 to+8.66. Unmineralized serpentinite, however, presents a very distinctive Nd isotopic composition at 0.512926 (ε_{Nd}=+5.62). This serpentinite exhibits the lowest ε_{Nd} and Co/Ni ratio for 1/Nd equal to 1. Stockwork samples exhibit low Co/Ni ratios (Co/Ni <1) and increasing ε_{Nd} values (+7.55 to +8.52) and 1/Nd ratios (1.91 to 8) while the semimassive sulfides show very

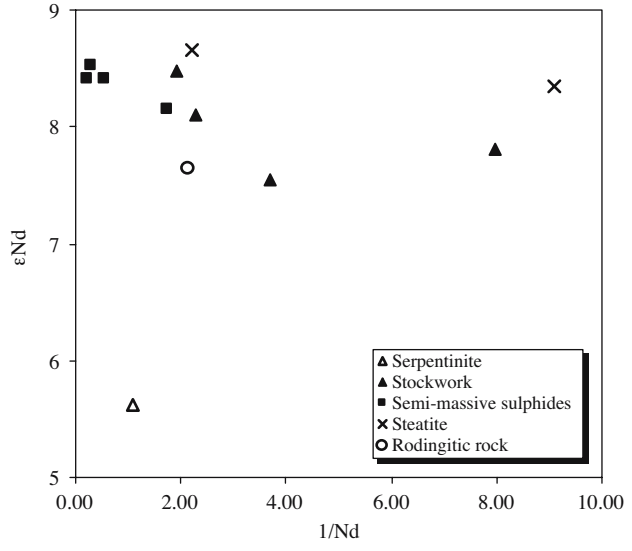

Fig. 9 εNd vs 1/Nd in selected samples from the Rainbow vent field

uniform ε_{Nd} values between +8.15 and +8.52 and high Co/Ni ratios (Co/Ni >5) and variable 1/Nd ratios (0.22–1.75) (Fig. 8). Rodingitic material and part of the stockwork exhibit lower ε_{Nd} and Co/Ni values when compared to the semimassive sulfides.

Discussion

Serpentinization and heat generation

Serpentine textures and mineralogy reveal that serpentinization has taken place at the subseafloor under low-temperature retrograde metamorphism. Olivine reacted first, and more extensively than pyroxene, producing pseudomorphic (lizardite-dominated) textures. Considering the latter observations, temperatures were certainly below 350°C (Moody 1976; Janecky and Seyfried 1986) and probably under 270°C (O'Hanley 1996; Allen and Seyfried 2004). Serpentinization reactions are exothermic (MacDonald and Fyfe 1985; Fyfe 1992; O'Hanley 1992; Kelley et al. 2001; Lowell and Rona 2002; Schroeder et al. 2002; Allen and Seyfried 2004) but are unlikely to produce hydrothermal temperatures above a few tens of degrees Celsius. To produce hydrothermal fluids slightly above 100°C, serpentinization rates need to be extremely high (100 Kg/s) and flow rates low (10 Kg/s) (Lowell and Rona 2002). At the Rainbow, the opposite occurs: flow rates are high (500 Kg/s) and serpentinization rates are probably low (~0.1 Kg/s) except when, episodically, new reaction surfaces are available (MacDonald and Fyfe 1985; Thurnherr and Richards 2001; Lowell and Rona 2002). Thus, it is extremely unlikely that serpentinization reactions alone can produce the reported high temperatures at the Rainbow vents. Furthermore, the hydrothermal sulfide mineralization event indisputably overprints the serpentinization event, thus, any considerations regarding the vent fluid properties cannot be directly attributed to serpentinization reactions alone. Consequently, the presence of a magmatic heat source at depth as previously proposed by several authors (Cave et al. 2002; Lowell and Rona 2002; Mével 2003; Allen and Seyfried 2004) prevails as a reasonable explanation.

Sulfide mineralization

Serpentinites are naturally Cu and Zn depleted but the textures and chemistry of the sulfide-bearing rocks found at Rainbow show conspicuous similarities with mafic VMS deposits. In accordance to this, the Rainbow massive sulfide ore-grade deposit is Cu- and Zn-rich (28wt% Cu, 5wt% Zn), but Pb depleted whereas the upper parts of the hydrothermal system are also extremely Co-enriched (up to ~6,300 ppm) with high Co/Ni ratios. These elements are characteristic of mafic-hosted seafloor hydrothermal systems. It is reasonable to assume that a mafic metal source is responsible for Cu, Zn, and Co input along with Fe into the system. Cu-Fe sulfide chemistry data suggest that temperature decreases from deeper stockwork through subsurface semimassive sulfides to MS-ch.

Ni and Co are remobilized during serpentinization from primary minerals into serpentinite-group minerals and later during sulfide mineralization into sulfides (Marques et al. 2003). While Ni gradually decreases, Co increases sharply with the evolution of the hydrothermal system (Srp–St–Stea and Srp–St–SMS–MS) indicating Co input. These observations apply both to bulk-rock and sulfide chemistry data. Co/Ni ratios were used as indicators to discriminate sulfide deposits of different settings. At Rainbow, Co/Ni ratios found in stockwork py compare well to those of py from the serpentinite-hosted Eastern Metals deposit (Auclair et al. 1993), whereas the Co-rich py with Co/Ni ratios >1 found in semimassive and massive sulfides match those of volcanogenic py found in VMS deposits from different localities (Loftus-Hills and Solomon 1967; Bralia et al. 1979; Mookherjee and Philip 1979; Walshe and Solomon 1981; Bajwah et al. 1987). Similar Co/Ni ratio variation was pointed out in the Outokumpu deposit ores with Co/Ni ratios typical of VMS deposits except for a few Ni-rich py found in the deeper parts of the deposit, which were interpreted as earlier sulfides (Loukola-Ruskeeniemi 1999).

In the Rainbow vent field, Co/Ni ratios seem to be excellent tools for discriminating between the various units.

LREE enrichment occurs alongside sulfide mineralization reaching a maximum in semimassive sulfides and decreasing again in the massive sulfide units. The presence of altered serpentinite relics in semimassive sulfides may favor the observed LREE retention. The REE-depleted character of the unmineralized serpentinites and the increasing LREE enrichment in the sulfide bearing rocks strongly suggest that the source of metals (Cu, Zn, and Fe) transported by the hydrothermal fluid should also contribute with LREE. HREE patterns are nearly constant throughout the system compatible with the higher LREE mobility as Cl complexes in acidic solutions (Mills and Elderfield 1995; Douville et al. 1999).

Nd isotopes

Hydrothermal fluids that were originally seawater were progressively modified via (direct or indirect) magmatic interactions during percolation. The sulfides formed during the hydrothermal sulfide mineralization episode acquired the Nd isotopic signature of the hydrothermal fluid from which they are derived. From the above sections, there is clear evidence that the sulfide-bearing serpentinites (stockwork and semimassive sulfides) and related rocks (steatites and rodingitic material) result from the same peridotite precursor as the serpentinite. However, it is the combination of the serpentinization process with the presence of a magmatic heat source at depth (e.g., intrusion of a gabbroic body) that may explain the chemical characteristics of the Rainbow site (Cave et al. 2002; Lowell and Rona 2002; Mével 2003; Allen and Seyfried 2004). The contribution of

two sources (seawater and magmatic) in the hydrothermal fluid at Rainbow is also supported by Nd isotopic compositions and Co/Ni and 1/Nd ratios (Figs. 8 and 9).

At the Rainbow vent field, mineralized samples are characterized by ε_{Nd} values of +7.55 to +8.66 but no Nd isotope ratios have so far been measured on Rainbow hydrothermal fluids. Basalts in the vicinity of the Rainbow vent site (South AMAR segment between 36.29 and 35.67°N) exhibit ε_{Nd} values at +8.56 to +9.95 ($^{143}Nd/^{144}Nd$=0.513077 to 0.513148), which correspond to the top end of our sample variation range (Figs. 8 and 9; Dosso et al. 1999). In contrast, the present day deep-water circulation in the Rainbow rift valley is characterized by an inflow of North East Atlantic Deep Water from the eastern ridge flank with ε_{Nd} value of −12.4 (Thurnherr and Richards 2001; Thurnherr et al. 2002; Lacan 2002). In comparison, the East Pacific Rise (EPR) hydrothermal fluids present ε_{Nd} values of +5 to +7 (Michard and Albarède 1986), lower by 2 ε_{Nd} values than those of the oceanic crust at that location. Mineralized rocks and oceanic crust from the Rainbow area exhibit similar ε_{Nd} variations to the EPR contrasting with the Nd isotope signature of the seawater within the area.

The low ε_{Nd} value of the unmineralized serpentinite probably results from simple peridotite–seawater interaction as supported by the low Co/Ni ratio (low Co/Ni ratio in peridotite and seawater, see Niu et al. 2001). Subsequently, a higher temperature hydrothermal fluid with high Co/Ni ratios and radiogenic Nd isotopic composition is gradually superimposed on the previous regime. This leads to the formation of sulfide mineralization during focused fluid upflow mainly under the seafloor. This would explain the mixing trend in the stockwork samples and rodingitic material that preserve characteristics of the earlier serpentinization-related fluid regime (low Co/Ni, unradiogenic Nd isotope) mixed with the later mineralizing fluid regime (high Co/Ni, radiogenic Nd isotopic composition). The nonmixing trend in the semimassive sulfides is generated by the high ε_{Nd} and Co/Ni values and low 1/Nd. The emplacement of a gabbroic body (with N-MORB affinity) within the serpentinites can provide heat and elements, which easily explain the isotope signatures and all other peculiarities found in the Rainbow vent field.

Vent fluid chemistry

Rainbow fluids hold the highest reported chloride concentration, the lowest end-member pH, high trace metal contents, and high REE, K, Rb, and Cs contents (Douville et al. 2002). Experiments on simple peridotite–seawater interactions at temperatures below 350°C produced high pH fluids (neutral to alkaline) rich in H_2, CH_4, H_2S, Mn, and SiO_2 with low dissolved metal contents (Seyfried and Dibble 1980, Berndt et al. 1996; Donval et al. 1997; Charlou et al. 2000; Kelley et al. 2001; Palandri and Reed 2004). At temperatures of ~400°C, fluids are initially acidic (pH increasing afterwards) with high dissolved Fe, Ca, and SiO_2 (Seyfried and Ding 1995; Allen and Seyfried 2003, 2004, 2005). Furthermore, Wetzel and Shock (2000) have calculated that simple peridotite–seawater interaction would produce a fluid with less than 50% K and ~95% SiO_2 than the fluid resulting from basalt–seawater reactions. These experiments could not reproduce the chemistry of the Rainbow vent fluids, most likely because they were based on the assumption that serpentinization occurs at high temperatures with olivine stable over pyroxene and antigorite as the stable serpentine phase.

On the other hand, experiments on basalt–seawater interactions at ~400°C produced a low pH fluid rich in metals (Fe > Mn > Zn > Cu), H_2S, LREE (La, Ce, and Eu), and CaO (Seyfried et al. 1986; Bischoff and Rosenbauer 1989; Bienvenu et al. 1990; Seewald and Seyfried 1990; Palandri and Reed 2004). These results are comparable to the composition of vent fluids from modern basalt-hosted high temperature systems and, remarkably, to the Rainbow vent field (Douville et al. 2002; James et al. 1995; Seewald and Seyfried 1990).

High mFe/mCu and mFe/mMn coupled with high Fe contents in the Rainbow vent fluids are indicative of reducing, acidic, and high temperature conditions at the subseafloor reaction zone. However, Zn content in fluids at temperatures >200°C do not seem to be temperature dependent (Seewald and Seyfried 1990; Large 1992; Hannington et al. 1995; Seyfried and Ding 1995; Charlou et al. 2000; Douville et al. 2002; Allen and Seyfried 2003). Thus the profusion of Zn in the Rainbow fluids is most probably related to source rock composition and/or brine/seawater mixing because there is no evidence for sp dissolution (Metz and Trefry 2000; Douville et al. 2002). The presence of Co is related to high temperature Cu-rich VMS deposits or even lower temperature fluids if chlorinity is high (e.g., Besshi-type VMS, Peter and Scott 1997).

The Rainbow end-member fluid is chlorine-rich (750 mM Cl)—surpassing seawater chlorinity (546 mM Cl) (Douville et al. 2002). The critical point for seawater is 407°C and 298.5 bars (Bischoff and Rosenbauer 1989) indicating that the Rainbow fluids venting at 365°C and 2,400 m depth have crossed the two-phase boundary below the critical point at minimum temperatures of 380°C (Charlou et al. 2000; Douville et al. 2002). Under subcritical conditions, boiling seems to be the predominant phase separation process causing the exsolution of volatile components (CO_2, H_2S, CH_4, SO_2, and H_2) into the vapor phase with drastic changes in the pH and fO_2 of the system (Drummond and Ohmoto 1985). Subcritical boiling results in only moderate increase in salinity (Charlou et al. 2000), which is possibly not enough to explain the high-chlorinity values at Rainbow. Under these conditions, mixing with high salinity brine or the direct magmatic contribution of a Cl-rich metal-bearing aqueous fluid would explain the high salinities and enriched metal contents.

Conclusions

Textural evidence of subseafloor hydrothermal replacement at the Rainbow vent field are indicative of a highly efficient process of trapping metals essential for the formation of an ore-grade deposit under the seafloor. The new geochemical data combined with the current knowledge at Rainbow presents compelling evidence for the presence of a gabbroic intrusion at depth contributing heat, metals, and other elements. The evolution of the system may be summarized as follows:

(1) A hot gabbroic body has intruded (near) a completely serpentinized peridotite.
(2) The resulting reaction zone is characterized by high temperature, acidic, and reducing conditions favoring metal leaching and efficient metal transport by Cl-rich hydrothermal fluids.
(3) The gabbroic body contributes heat and metals to sustain the hydrothermal circulation and provide the mafic VMS character of the sulfide deposit.
(4) Strongly positive CH_4 anomalies represent contributions from secondary peridotite–seawater reactions in the surrounding areas.

Acknowledgements The authors wish to thank Claudio Cermignani (University of Toronto) for technical and analytical support with the EPMA and Prof. Martin Sinha (NOC), Gabriela Henriques, and Yannick Beaudoin for improving the English. The manuscript benefited significantly from constructive comments and suggestions from Bernd Lehmann. Fundação Para a Ciência e Tecnologia (FCT) provided funds for the study through Project SEAHMA (FFCUL/FCT-PDCTM/P/MAR/15281/1999) and a Ph.D. scholarship (SFRH/BD/2978/2000) given to A. F. A. Marques. A. F. A. Marques also benefited from a student research grant from the Society of Economic Geologists Foundation. V. Chavagnac was funded by the 2000 National Oceanography Centre, Southampton Research Fellowship. The NERC core strategic science funds the hydrothermal research at NOCS.

References

Allen D, Seyfried WE Jr (2003) Alteration and mass transfer in the MgO-CaO-FeO-Fe2O3-SiO2-Na2O-H2O-HCl system at 400°C and 500 bars: implications for pH and compositional controls on vent fluids from ultramafic-hosted hydrothermal systems at mid-ocean ridges. Geochim Cosmochim Acta 67:1531–1542

Allen D, Seyfried WE Jr (2004) Serpentinization and heat generation: constraints from Lost City and Rainbow hydrothermal systems. Geochim Cosmochim Acta 67:1347–1354

Allen D, Seyfried WE Jr (2005) REE controls in ultramafic hosted MOR hydrothermal systems: an experimental study at elevated temperature and pressure. Geochim Cosmochim Acta 69:675–683

Alt JC (1995) Subseafloor processes in the mid-ocean ridge hydrothermal systems. In: Humphris SE, Zierenberg RA, Mullineaux LS, Thomson RE (eds) Seafloor hydrothermal systems: physical, chemical, biological and geological interactions. Geophys Monogr 91:85–113 (American Geophysical Union)

Alt JC, Shanks WC (2003) Serpentinization of abyssal peridotites from the MARK area, Mid-Atlantic Ridge: sulfur geochemistry and reaction modelling. Geochim Cosmochim Acta 67:641–653

Auclair M, Gauthier M, Trottier J, Jébrak M, Chartrand F (1993) Mineralogy, geochemistry, and paragenesis of the Eastern Metals serpentinite-associated Ni-Cu-Zn deposit, Quebec Appalachians. Econ Geol 88:123–138

Bajwah ZU, Seccombe PK, Offler R (1987) Trace element distribution, Co:Ni ratios and genesis of the Big Cadia iron–copper deposit, New South Wales, Australia. Miner Depos 22:292–300

Baker ET, German CR (2004) On the global distribution of mid-ocean ridge hydrothermal vent-fields. In: German CR, Lin J, Parson LM (eds) The thermal structure of the oceanic crust and the dynamics of seafloor hydrothermal circulation. Geophys Monogr 148:245–266 (American Geophysical Union)

Barrie CT, Hannington MD (1997) Introduction: classification of VMS deposits based on host rock composition. In: Barrie CT, Hannington MD (eds) Volcanic-associated massive sulfide deposits: processes and examples in modern and ancient settings. SEG 8:1–12 (Ottawa)

Barriga FJAS, Costa IMA, Relvas JMR, Ribeiro A, Fouquet Y, Ondréas H, Parson L, FLORES Scientific Party (1997) The Rainbow serpentinites and serpentinite-sulphide stock work (Mid-Atlantic Ridge, AMAR segment): a preliminary report of the FLORES results. EOS Abst 78:832

Barriga FJAS, Fouquet Y, Almeida A, Biscoito M, Charlou JL, Costa RLP, Dias A, Marques AMSF, Miranda JM, Olu K, Porteiro F, Queiroz M (1998) Discovery of the Saldanha hydrothermal field on the FAMOUS segment of the MAR (36°30′N). AGU fall meeting 1998. EOS Abst 79(45):F67

Barriga FJAS, Dias A, Marques AFA, Relvas JMRS, Miranda JM, Queiroz G, Lourenço N, Ferreira A, Fouquet Y, Iyer S, Saldanha Team, Seahma1 Team (2004) Mount Saldanha revisited: low-temperature methane discharge through a sediment-capped serpentinite protrusion (MoMAR Area, Mid-Atlantic Ridge, 36°30′N). In: EGU 1st General Assembly. Nice, France (25–30 April 2004)

Batuyev BN, Krotov AG, Markov VF, Cherkashev G, Krasnov SG, Lisitsyn Y (1994) Massive sulfide deposits discovered and sampled at 14°45′N, Mid-Atlantic Ridge. BRIDGE newsl 6:6–10

Bralia A, Sabatini G, Troja F (1979) A re-evaluation of the Co/Ni ratio in pyrite as geochemical tool in ore genesis problems. Miner Depos 14:353–374

Berndt ME, Allen DE, Seyfried WE Jr (1996) Reduction of CO_2 during serpentinization of olivine at 300° and 500 bar. Geology 24(4):351–354

Bienvenu P, Bougault H, Joron JL, Treuil M, Dmitriev L (1990) MORB alteration: rare earth element/non-rare-earth hygromagmaphile element fractionation. Chem Geol 82:1–14

Bischoff JL, Rosenbauer RJ (1989) Salinity variations in submarine hydrothermal systems by layered double-diffusive convection. J Geol 97:613–623

Bogdanov Y, Sagalevitch AM, Chernayev ES, Ashadze AM, Gurvich EZ, Lukashin VN, Ivanov GV, Peresypkin VN (1995) A study of the hydrothermal field at 14°45′N on the Mid-Atlantic Ridge using the "MIR" submersibles. BRIDGE newsl 9:9–13

Cave RR, German C, Thomson J, Nesbitt RW (2002) Fluxes to sediments underlying the Rainbow hydrothermal plume at 36°14′N on the Mid-Atlantic Ridge. Geochim Cosmochim Acta 66:1905–1923

Charlou JL, Donval JP, Douville E, Jean-Baptiste P, Radford-Knoery J, Fouquet Y, Dapoigny A, Stievenard M (2000) Compared geochemical signatures and the evolution of Menez Gwen (37°50′N) and Lucky Strike (37°17′N) hydrothermal fluids, south of the Azores triple junction on the Mid-Atlantic Ridge. Chem Geol 171:49–75

Chavagnac V, German C, Milton A, Palmer MR (2005) Sources of REE in sediment cores from the Rainbow vent site (36°14′N, MAR). Chem Geol 216:329–352

Costa I (2005) Serpentinization on the Mid-Atlantic Ridge: Rainbow, Saldanha and Menez Hom Sites. Ph.D. thesis, Dep. Geologia, Universidade de Lisboa, p 400

Donval JP, Charlou JL, Douville E, Knoery J, Fouquet Y, Ponseveras E, Baptiste PJ, Stievenard M, German C, FLORES Scientific Party (1997) High H_2 and CH_4 content in hydrothermal fluids from Rainbow site newly sampled at 36°14′N on the AMAR segment, Mid-Atlantic Ridge (diving FLORES cruise, July 1997). Comparison with other MAR sites. EOS Abst 78:832

Dosso L, Bougault H, Langmuir C, Bollinger C, Bonnier O, Etoubleau J (1999) The age and distribution of mantle heterogeneity along the Mid-Atlantic Ridge (31–41°N). Earth Planet Sci Lett 170:269–286

Douville E, Bienvenu P, Charlou JL, Donval JP, Fouquet Y, Appriou P, Gamo T (1999) Yttrium and rare earth elements in fluids from various deep-sea hydrothermal systems. Geochim Cosmochim Acta 63:627–643

Douville E, Charlou JL, Donval JP, Knoery J, Fouquet Y, Bienvenu P, Appriou P, FLORES Scientific Party (1997) Trace elements in fluids from the new Rainbow hydrothermal field (36°14′N, MAR): a comparison with other Mid-Atlantic Ridge fluids. EOS Abst 78:832

Douville E, Charlou JL, Oelkers EH, Bienvenu P, Jove Colon CF, Donval JP, Fouquet Y, Prieur D, Appriou P (2002) The Rainbow vent fluids (36°14′N, MAR): the influence of ultramafic rocks and phase separation on trace metal content in Mid-Atlantic Ridge hydrothermal fluids. Chem Geol 184:37–48

Doyle M, Allen R (2003) Subsea-floor replacement in volcanic-hosted massive sulfide deposits. Ore Geol Rev 23:183–222

Drummond SE, Ohmoto H (1985) Chemical evolution and mineral deposition in boiling hydrothermal systems. Econ Geol 80:126–147

Edmonds HN, German C (2004) Particle geochemistry in the Rainbow hydrothermal plume, Mid-Atlantic Ridge. Geochim Cosmochim Acta 68:759–772

FLORES Cruise Report (1998) IFREMER, France

Fouquet Y, Stackelberg U, Charlou JL, Erzinger J, Herzig PM, Mühe R, Wiedicke M (1993a) Metallogenesis in back-arc environments: the Lau Basin example. Econ Geol 88:2154–2181

Fouquet Y, Wafik A, Cambon P, Mevel C, Meyer G, Gente P (1993b) Tectonic setting and mineralogical and geochemical zonation in the Snake Pit sulfide deposit (Mid-Atlantic Ridge at 23°N). Econ Geol 88:2018–2036

Fouquet Y, Knott R, Cambon P, Fallick A, Rickard D, Desbruyeres D (1996) Formation of large sulfide mineral deposits along fast spreading ridges. Example from off-axial deposits at 12°43′N on the East Pacific Rise. Earth Planet Sci Lett 144:147–162

Fouquet Y, Charlou JL, Ondreas H, Radford-Knoery J, Donval JP, Douville E, Appriou al R, Cambon P, Pellé H, Landuré JY, Normand A, Ponsevera E, German C, Parson L, Barriga F, Costa I, Relvas J, Ribeiro A (1997) Discovery and first submersible investigations on the Rainbow hydrothermal field on the MAR (36°14N) AGU fall meeting 1997. EOS Abst 78 (46)-Supl-F832

Früh-Green G, Kelley DS, Bernasconi SM, Karson JA, Ludwig KA, Butterfield DA, Boschi C, Proskurowski G (2003) 30000 years of hydrothermal activity at the Lost City vent field. Science 301:495–498

Fyfe WS (1992) Geosphere interactions on a convecting planet: mixing and separation. In: Hutzinger O (ed) The handbook of environmental chemistry 1. Springer, Berlin Heidelberg New York, pp 1–26

German C, Higgs NC, Thomson J, Mills RA, Elderfield H, Blusztajn J, Fleer AP, Bacon MP (1993) A geochemical study of metalliferous sediment from the TAG hydrothermal mound 26°08′N Mid-Atlantic Ridge. J Geophys Res 98:9683–9692

German C, Klinkhammer CP, Rudnicki MD (1996) The Rainbow hydrothermal plume, 36°15′N, MAR. Geophys Res Lett 23 (21):2979–2982

Goodfellow WD, Franklin JM (1993) Geology, mineralogy, and chemistry of sediment-hosted clastic massive sulfides in shallow cores, Middle Valley, Northern Juan de Fuca Ridge. Econ Geol 88:2037–2068

Gràcia E, Charlou JL, Knoery J, Parson LM (2000) Non-transform offsets along the Mid-Atlantic Ridge south of the Azores (38° N–34°N): ultramafic exposures and hosting of hydrothermal vents. Earth Planet Sci Lett 177:89–109

Hannington MD, Jonasson IR, Herzig PM, Petersen S (1995) Physical and chemical processes of seafloor mineralization at mid-ocean ridges. In: Humphris SE, Zierenberg RA, Mullineaux LS, Thomson RE (eds) Seafloor hydrothermal systems: physical, chemical, biological and geological interactions. Geophys Monogr 91:466 (American Geophysical Union)

Hawley JE, Nichol I (1961) Trace elements in pyrite, pyrrhotite and chalcopyrite of different ores. Econ Geol 56:467–487

Herzig PM, Hannington MD (1995) Polymetallic massive sulfides at the modern seafloor. A review. Ore Geol Rev 10:95–115

Herzig PM, Petersen S, Hannington MD (1998) Geochemistry and sulphur-isotopic composition of the TAG hydrothermal mound, Mid-Atlantic Ridge, 26°N. In: Herzig PM, Humphris SE, Miller DJ, Zierenberg RA (eds) Proceedings of the ocean drilling program scientific results 158:47–70

Humphris SE, Herzig PM, Miller S, Alt JC, Becker K, Brown D, Brügmann G, Chiba H, Fouquet Y, Gemmell JB, Guerin JB, Hannington MD, Holm MD, Honnorez J, Iturrino JJ, Knott GJ, Ludwig R, Nakamura K, Petersen S, Reysenbach A, Rona PA, Smith D, Sturz A, Tivey MK, Zhao X (1995) The internal structure of an active seafloor massive sulphide deposit. Nature 377:713–716

Huston DL, Sie SH, Suter GF (1995) Selenium and its importance to the study of ore genesis: the theoretical basis and its application to volcanic-hosted massive sulfide deposits using pixeprobe analysis. Nucl Instrum Methods Phys Res B 104:476–480

Hutchinson MN, Scott SD (1981) Sphalerite geobarometry in the Cu-Fe-Zn-S system. Econ Geol 76:143–153

IRIS Cruise Report (2001) IFREMER, France

James RH, Elderfield H, Palmer MR (1995) The chemistry of hydrothermal fluids from the Broken Spur site, 29°N Mid-Atlantic Ridge. Geochim Cosmochim Acta 59:651–659

Janecky DR, Seyfried WE Jr (1986) Hydrothermal serpentinization of peridotite within the oceanic crust: experimental investigations of mineralogy and major element chemistry. Geochim Cosmochim Acta 50:1357–1378

Kase K, Yamamoto M, Shibata T (1990) Copper-rich sulfide deposit near 23°N, Mid-Atlantic Ridge: chemical composition, mineral chemistry, and sulphur isotopes. In: Detrick R, Honnorez J, Bryan WB, Juteau T (eds) Proceedings of the ocean drilling program scientific results, pp 163–175

Kelley D, Karson JA, Blackman DK, Früh-Green GL, Butterfield D, Lilley MD, Olson E, Schrenk M, Roe K, Lebon GT, Rivizzigo P, AT3-60 scientific party (2001) An off-axis hydrothermal vent field near the Mid-Atlantic Ridge at 30°N. Nature 412:145–149

Kojima S, Sugaki A (1985) Phase relations in the Cu-Fe-Zn-S System between 500° and 300° under hydrothermal conditions. Econ Geol 80:158–171

Lacan F (2002) Masses d'eau des mers nordiques et de l'Atlantique subarctique tracées par les isotopes du néodyme Laboratoire des études géophysiques et océanographiques spatiales. Université Toulouse III, Paul Sabatier, Toulouse, pp 293

Langmuir C, Humphris SE, Fornari DJ, Van Dover C, Von Damm KL, Tivey MK, Colodner D, Charlou JL, Desonie D, Wilson C, Fouquet Y, Klinkhammer G, Bougault H (1997) Hydrothermal vents near a mantle hot spot: the Lucky Strike vent field at 37′N on the Mid-Atlantic Ridge. Earth Planet Sci Lett 148:69–91

Large R (1992) Australian volcanic-hosted massive sulfide deposits: features, styles, and genetic models. Econ Geol 87:471–510

Lawrie D, Miller DJ (2000) Data report: sulfide mineral chemistry and petrography from Bent Hill, ODP Mound and TAG massive sulfide deposits. In: Zierenberg RA, Fouquet Y, Miller DJ, Normak WR (eds) Proceedings of the ocean drilling program scientific results, pp 1–34

Lein AY, Ulyanova NV, Ulyanov A, Cherkashev ä, Stepanova T (2001) Mineralogy and geochemistry of sulfide ores in ocean-floor hydrothermal fields associated with serpentine protrusions. Rus J Earth Sci 3(5)

Loftus-Hills G, Solomon M (1967) Cobalt, nickel and selenium in sulphides as indicators of ore genesis. Miner Depos 2:228–242

Loukola-Ruskeeniemi K (1999) Origin of black shales at the serpentinite-associated Cu-Zn-Co ores at Outokumpu, Finland. Econ Geol 94:1007–1028

Lowell RP, Rona PA (2002) Seafloor hydrothermal systems driven by the serpentinization of peridotite. Geophys Res Lett 29: 26-1–26-4

Marques AFA, Barriga FJAS, Fouquet Y (2003) Co:Ni ratio variation throughout the Rainbow hydrothermal system. In: Eliopoulos DG et al (eds) Mineral exploration and sustainable development. Proceedings of the Seventh Biennial SGA Meeting, Athens, Greece, 24–28 August 2003. Millpress, Rotterdam, pp 143–146

MacDonald AM, Fyfe WS (1985) Rate of serpentinization in seafloor environments. Tectonophysics 116:123–135

McDonough WF, Sun S (1995) The composition of the Earth. Chem Geol 120:223–253

Metz S, Trefry JH (2000) Chemical and mineralogical influences on concentrations of trace metals in hydrothermal fluids. Geochim Cosmochim Acta 64:2267–2279

Mével C (2003) Serpentinization of abyssal peridotites at mid-ocean ridges. CR Geoscience 335:825–852

Michard A, Albarède F (1986) The REE content of some hydrothermal fluids. Chem Geol 55:51–60

Mills RA, Elderfield H (1995) Rare earth element geochemistry of hydrothermal deposits from the active TAG mound, 26° north, Mid-Atlantic Ridge. Geochim Cosmochim Acta 59:3511–3524

Moody JB (1976) Serpentinization: a review. Lithos 9:125–138

Mookherjee A, Philip R (1979) Distribution of copper, cobalt and nickel in ores and host rocks, Ingladhol, Karhataka, India. Miner Depos 14:33–55

Münch U, Blum N, Halbach P (1999) Mineralogical and geochemical features of sulfides from the MESO zone, Central Indian Ridge. Chem Geol 155:29–44

Niu Y, Bideau D, Hekinian R, Batiza R (2001) Mantle compositional control on the extent of mantle melting crust production, gravity anomaly, ridge morphology, and ridge segmentation: a case study at the Mid-Atlantic Ridge 33–35°N. Earth Planet Sci Lett 186:383–399

O'Hanley DS (1992) Solution to the volume problem in serpentinization. Geology 20:705–708

O'Hanley DS (1996) Serpentinites. Records of tectonics and petrological history. Oxford Univ. Press, New York, p 277

Palandri JL, Reed MH (2004) Geochemical models of metasomatism in ultramafic systems: serpentinization, rodingitization, and sea floor carbonate chimney precipitation. Geochim Cosmochim Acta 68:1115–1133

Parson L, Fouquet Y, Ondréas H, Barriga FJAS, Relvas JMR, Ribeiro A, Charlou JL, German C, FLORES Scientific Party (1997) Non-transform discontinuity settings for contrasting hydrothermal systems on the MAR-Rainbow and FAMOUS at 36°14′ and 36°34′N. EOS Abst 78:832

Peter J, Scott SD (1997) Windy Craggy, northwestern British Columbia: the world's largest Besshi-type deposit. In: Barrie CT, Hannington MD (eds) Volcanic associated massive sulfide deposits: processes and examples in modern and ancient settings. Rev Econ Geol 8:261–295

Rona PA, Hannington MD, Raman CV, Thompson G, Tivey MK, Humphris SE, Lalou C, Petersen S (1993) Active and relic seafloor hydrothermal mineralization at the TAG hydrothermal field, Mid-Atlantic Ridge. Econ Geol 88:1989–2017

SALDANHA Cruise Report (1999) Universidade de Lisboa, Portugal

Saunders AD, Norry MJ, Tarney J (1988) Origin of MORB and chemically depleted mantle. J Petrol (Special Lithosphere Issue):415–445

Seewald JS, Seyfried WE Jr (1990) The effect of temperature on metal mobility in sub seafloor hydrothermal systems: constraints from basalt alteration experiments. Earth Planet Sci Lett 101:388–403

SEAHMA Cruise Report (2003) Universidade de Lisboa, Portugal

Seyfried WE Jr, Dibble WE Jr (1980) Seawater-peridotite interaction at 300° C and 500 bars: implications for the origin of oceanic serpentinites. Geochim Cosmochim Acta 44:309–321

Seyfried WE Jr, Berndt ME, Janecky D (1986) Chloride depletions and enrichments in seafloor hydrothermal fluids: constraints from experimental basalt alteration studies. Geochim Cosmochim Acta 50:469–475

Seyfried WE Jr, Ding K (1995) Phase equilibria in sub seafloor hydrothermal systems: a review of the role of redox, temperature, pH and dissolved Cl on the chemistry of hot spring fluids at mid-ocean ridges. In: Humphris SE, Zierenberg RA, Mullineaux LS, Thomson RE (eds) Seafloor hydrothermal systems: physical, chemical, biological and geological interactions. Geophys Monogr 91:248–272 (American Geophysical Union)

Schroeder T, John B, Frost B (2002) Geologic, implications of seawater circulation through peridotite exposed at slow-spreading mid-ocean ridges. Geology 30:367–370

Thurnherr AM, Richards KJ (2001) Hydrography and high-temperature heat flux of the Rainbow hydrothermal site (36°14′N, Mid-Atlantic Ridge). J Geophys Res 106:9411–9426

Thurnherr AM, Richards KJ, German CR, Lane-Serff GF, Speer KG (2002) Flow and mixing in the rift valley of the Mid-Atalntic Ridge. J Phys Ocean 132:1763–1778

Tivey MK, Humphris SE, Thompson G, Hannington MD, Rona PA (1995) Deducing patterns of fluid flow and mixing within the active TAG hydrothermal mound using mineralogical and geochemical data. J Geophys Res 100:12527–12555

Vaughan DJ, Craig JR (1997) Sulfide ore stabilities, morphologies and intergrowth textures. In: Barnes HL (ed) Geochemistry of hydrothermal ore deposits (3rd edn). Wiley, New York, pp 367–434

Walshe JL, Solomon M (1981) An investigation into the environment of formation of the volcanic-hosted Mt. Lyell copper deposits using geology, mineralogy, stable isotopes and a six component chlorite solid solution model. Econ Geol 76:246–280

Wetzel L, Shock EL (2000) Distinguishing ultramafic from basalt hosted submarine hydrothermal systems by comparing calculated vent fluid compositions. J Geophys Res 105:8319–8340